Available online at www.sciencedirect.com
SCIENCE DIRECT®
ELSEVIER
Journal of Magnetism and Magnetic Materials 293 (2005) 28–32
Journal of magnetism and magnetic materials
www.elsevier.com/locate/jmmm

Amorphous magnetic microspheres for biomedical applications

Horia Chiriac[a,*], Anca-Eugenia Moga[a], Gheorghe Iacob[b], Ostin C. Mungiu[b]

[a]*National Institute of Research and Development for Technical Physics, 47 Mangeron Boulevard, R-700050 Iasi, Romania*
[b]*"Gr. T. Popa" University of Medicine and Pharmacy, R-700115 Iasi, Romania*

Available online 2 March 2005

Abstract

The method of preparation and physical properties of $Co_{68.25}Fe_{4.5}Si_{12.25}B_{15}$ amorphous microspheres, with special emphasis on the magnetic ones, are presented. Tissue tolerance was tested on Wistar white rats, and the results suggest that these amorphous magnetic microspheres are potential candidates for biomedical applications.

Keywords: Amorphous magnetic microspheres; Gas–liquid atomization; Biomedical applications; Tissue tolerance; Wistar rat; Toxicity; Cobalt; CoFeSiB; Nozzle; Preparation method

Currently, there are few magnetic materials used as magnetic micro and nanocarriers in biomedical and biotechnological applications. Fe oxides, and especially magnetite (Fe_3O_4), are mostly used in such applications, either as a background material for magnetic fluids or as magnetic particles, covered or not with a thin layer of polymer or other biocompatible materials [1]. Amorphous magnetic materials, both as micro and nanoparticles, could be successfully used as magnetic carriers because of their specific magnetic properties.

Usually, the transition metal–metalloid amorphous alloys are obtained by melt-spinning method at cooling rates of 10^5–10^6 K/s in order to avoid the crystallization onset and to preserve the disordered amorphous structure. Most of these materials are corrosion resistant, mechanically hard, but magnetically very soft [2]. The amorphous magnetic alloys of practical interest are usually available under the shape of splats, thin foils, ribbons, wires, glass-covered micro-wires or powders obtained by milling the amorphous ribbons.

Among the different techniques, it has been shown that the efficient methods and with higher reproducibility to obtain amorphous powders are the gas and gas–liquid atomization [3]. The

*Corresponding author. Tel.: +40 32 130680; fax: +40 32 231132.
E-mail address: hchiriac@phys-iasi.ro (H. Chiriac).

0304-8853/$ - see front matter © 2005 Elsevier B.V. All rights reserved.
doi:10.1016/j.jmmm.2005.01.039

atomization fluids (argon/nitrogen and water) disrupt the stream of liquid metal into droplets, which are quenched in a stream of gas or gas and water. Powders obtained by these methods are mostly spherical, the amorphous fraction being larger when the particle dimensions are smaller.

In this paper, we report some of our recent results concerning the preparation, properties and potential biomedical applications of $Co_{68.25}Fe_{4.5}Si_{12.25}B_{15}$ amorphous magnetic microspheres (AMMS) prepared by gas–liquid atomization technique.

The schematic diagram of our home-made gas–liquid atomization device used to prepare AMMS [4] is presented in Fig. 1.

$Co_{68.25}Fe_{4.5}Si_{12.25}B_{15}$ master alloys have been prepared by induction melting a mixture of Co, Fe, B, and Si crystalline pieces with purities over 99.9%. The alloys have been re-melted several times to ensure the compositional homogeneity. Pieces from the master alloy have been placed into a quartz crucible and overheated up to 1250–1300 °C and then released through a nozzle by applying an argon over-pressure of about 6 atm. The liquid metal stream was directed to the atomizer where it was disrupted into droplets and quenched by the combined gas and water jets. The method assures high quench rates of 10^5–10^6 K/s and consequently allows the successful preparation of AMMS.

The atomization process as well as the shape, the dimensions and the fraction of the amorphous phase are strongly influenced by the following technological parameters: the diameter of the nozzle, the temperature of the molten alloy, the angles between the gas, liquid atomizers and the fixing support, the distance between the nozzle and the atomizer, the pressure of fluids jets.

The above-mentioned atomization device was used to prepare 12 experimental batches of AMMS of 3–8 g each. The samples have been prepared using different technological parameters, in order to establish the suitable conditions for the preparation of a large percentage of spherical particles with smaller dimensions. The size distribution of the atomized powders was measured by using different sieves with various dimensions.

The morphology and the size of the AMMS have been put in evidence by means of scanning electron microscopy (SEM). Fig. 2 shows the SEM micrograph of the $Co_{68.25}Fe_{4.5}Si_{12.25}B_{15}$ AMMS. One can observe that most AMMS are spherical, but there is also a small fraction of ellipsoidal particles. However, their surface is perfectly round, without any asperities or discontinuities.

Most spherical AMMS were obtained under the following conditions: (a) nozzle diameters, d, of 91, 111, 135 and 160 μm; (b) molten alloy temperature T_m of 1250–1300 °C; (c) nozzle to atomizer

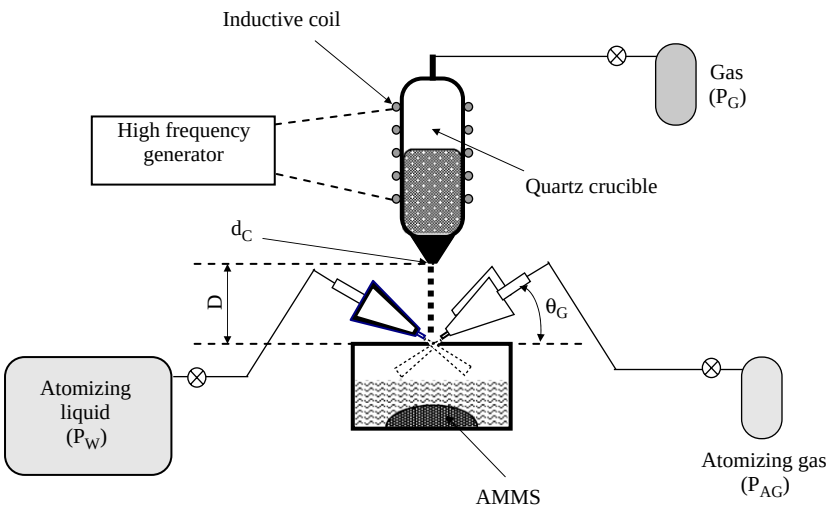

Fig. 1. The schematic diagram of the gas–liquid atomization device used for the AMMS preparation.

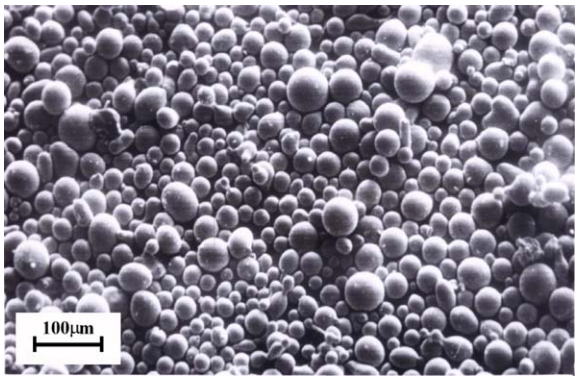

Fig. 2. SEM micrograph of $Co_{68.25}Fe_{4.5}Si_{12.25}B_{15}$ AMMS.

distance D of 8–15 mm; (d) ejection pressure applied on the molten alloy P_{AM} of 6–7.5 atm; (e) atomization gas pressure P_N of 6–8 atm; and (f) water pressure P_W of 2.8–3 atm.

The smaller AMMS were produced for a nozzle diameter of 91 μm. The decrease of the nozzle diameter determines the increase of both the ejection pressure applied on the molten alloy and the molten alloy temperature. If this correlation is not considered, the AMMS cannot be obtained spherical anymore, but ellipsoidal or as filaments fragments. A fraction of about 72% from the microspheres total mass has dimensions between 150 and 300 μm for a quartz crucible nozzle diameter $d = 160$ μm. For a nozzle diameter $d =$ 91 μm, the microparticles have sizes between 5 and 150 μm, from which a mass fraction of about 78% has dimensions between 26 and 60 μm.

The size distribution of the atomized magnetic microspheres for a diameter nozzle of 91 μm is presented in Fig. 3. Whereas in Fig. 4 the size distribution of the atomized magnetic microspheres for a diameter nozzle of 160 μm is shown.

The density of the AMMS was measured for six batches obtained in different conditions, the value being $(6.9 \pm 0.2) \times 10^3$ kg/m^3. The density decreases to $(5.8–6.5) \times 10^3$ kg/m^3 for microspheres larger than 300 μm, probably due to their inhomogeneous structure (gas microinclusions).

The structure of the AMMS was examined by X-ray diffraction (XRD) using MoKα radiation ($\lambda = 0.71069$ Å). Fig. 5 shows the XRD patterns of $Co_{68.25}Fe_{4.5}Si_{12.25}B_{15}$ AMMS with sizes < 100 μm

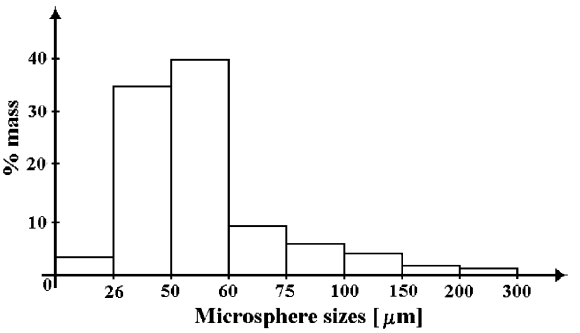

Fig. 3. Size distribution of atomized magnetic microspheres for a quartz crucible with a nozzle diameter of 91 μm.

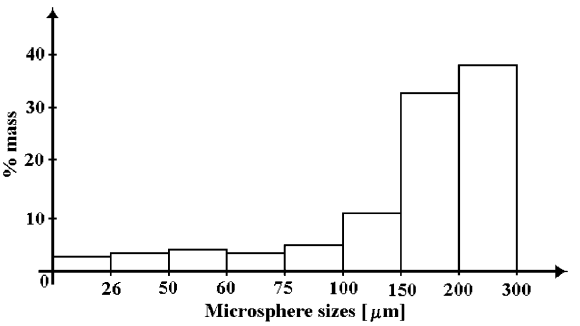

Fig. 4. Size distribution of atomized magnetic microspheres for a quartz crucible with a nozzle diameter of 160 μm.

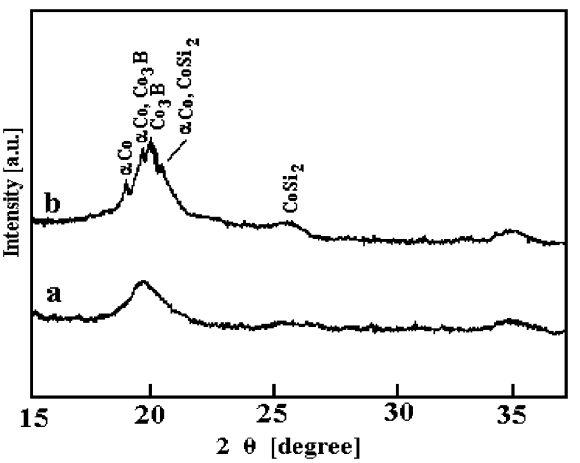

Fig. 5. XRD patterns of $Co_{68.25}Fe_{4.5}Si_{12.25}B_{15}$ AMMS: < 100 μm (a) and between 100 and 300 μm (b).

(a) and sizes between 100 and 300 μm (b). For the AMMS with sizes < 100 μm only one broad peak appears, indicating the existence of a fully amorphous phase. For the AMMS with sizes between 100 and 300 μm one observes a partially crystallized structure, with sharp diffraction peaks corresponding to α-Co, Co_3B and $CoSi_2$ crystalline phases superimposed on the broad maximum of the amorphous phase. The precipitation of crystalline phases is caused by the inhomogeneous cooling and the melt undercooling prior to the solidification.

The thermal stability of the AMMS was investigated by means of differential thermal analysis (DTA) combined with differential thermo-magneto gravimetry analysis (DTMG), at a heating rate of 10 °C/min. The DTA curves are presented in Fig. 6. One can observe the existence of only one exothermic peak at 545 °C, indicating one stage crystallization process for $Co_{68.25}Fe_{4.5}Si_{12.25}B_{15}$ AMMS. The increase of the signal at temperatures below 410 °C, just before the onset of the crystallization, may be due to either the oxidation or the rearrangements of the atoms in their equilibrium positions during the relaxation of the amorphous phase. During the crystallization, the amorphous structure evolves into a mixture of α-Co (Fe,Si), borides (Co_3B, Co_2B) and silicides ($CoSi_2$). The energy of crystallization for AMMS particles of 100–300 μm (b) is smaller than that of the particles below 100 μm (a), due to the coexistence of the amorphous and crystalline phases in the as-cast state, in agreement with the XRD results presented in Fig. 5. The Curie temperature of the AMMS was determined from the DTMG curves as being $T_C = 345 \pm 2$ °C.

Room temperature magnetic characteristics of the AMMS were determined by using a vibrating sample magnetometer (VSM), in an external field of 15 kOe. Fig. 7 shows the variation of the saturation magnetization and the coercive field as a function of the particle sizes for the atomized magnetic microspheres obtained for a diameter nozzle of 91 μm. The saturation magnetization and the coercive field of the atomized microspheres with sizes between 26 and 300 μm range between 79.8 and 42 emu/g and 305 and 384 Oe, respectively. The saturation magnetization decreases when the microspheres size increases from 26 to 300 μm, whereas the coercive field increases with the increase of the AMSS size due probably to the precipitation of some non-magnetic phases.

The magnetic measurements performed for 10 batches of AMMS indicate the following minimum and maximum values of the coercive field, saturation magnetization and remanence, respectively: $H_{C,min} = 329$ Oe; $H_{C,max} = 367$ Oe; $M_{S,min} = 51$ emu/g; $M_{S,max} = 71.5$ emu/g; $M_{R,min} = 6.6$ emu/g; $M_{R,max} = 10.7$ emu/g. Fig. 8 shows the magnetic hysteresis loops for AMMS of 100 μm, obtained for diameter nozzles of 91 (a) and 111 μm (b), respectively. The mechanism responsible for the 2 different hysteresis loops is the nonuniform

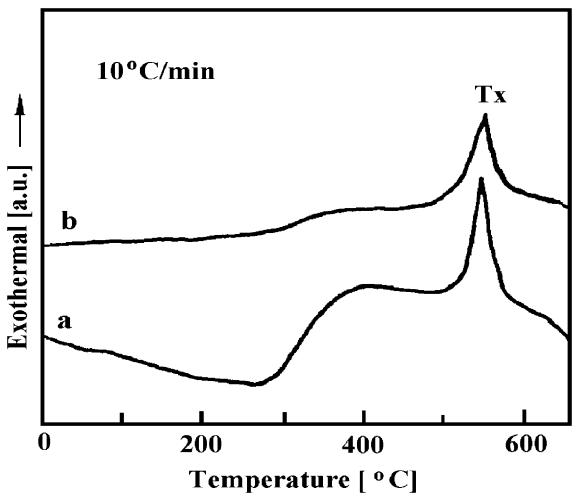

Fig. 6. DTA curves of $Co_{68.25}Fe_{4.5}Si_{12.25}B_{15}$ AMMS: < 100 μm (a) and between 100 and 300 μm (b).

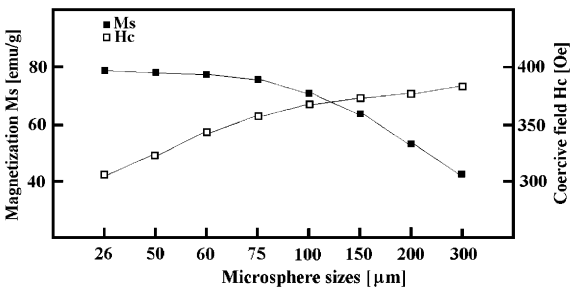

Fig. 7. Variation of the saturation magnetization and the coercive field of the AMMS vs. particle sizes, at room temperature.

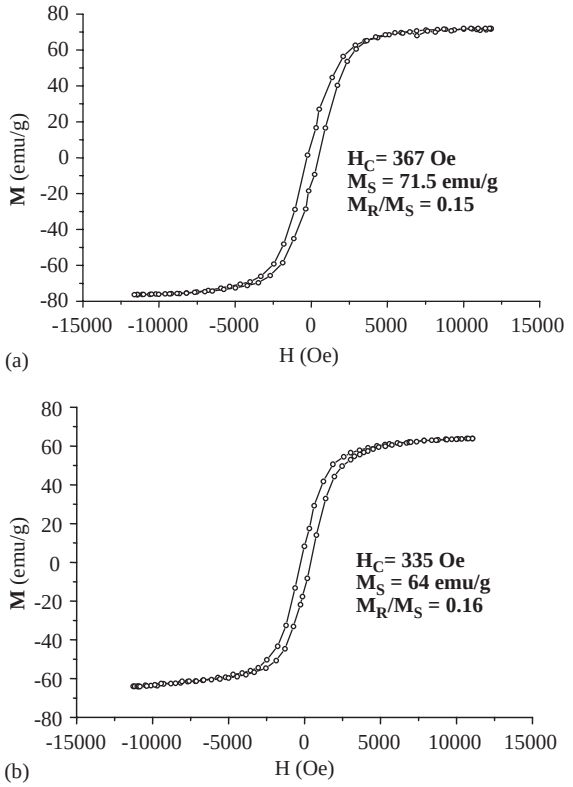

Fig. 8. Magnetic hysteresis loops for AMMS, obtained for quartz crucible diameter nozzles of 91 (a) and 111 μm (b).

cooling of the melt prior to the solidification, which induces different metastable phases in the obtained microspheres.

The tissue tolerance of the amorphous magnetic microspheres AMMS was tested, in standard laboratory conditions, on two groups of 20 Wistar white rats weighing 150 ± 20 g. For each rat, 100 mg of microspheres were introduced subcutaneously in the interscapular region, followed by observation for 14 days (first group) and 45 days (second group).

The tissue tolerance was studied by histopatologic observations of epidermis, dermis, hipodermis and muscular tissue.

By direct observation and anathomo-pathological investigation it was established that the microspheres do not induce inflammation processes or other local intolerance symptoms. This is due likely to the chemical inertia of the amorphous alloy from which the magnetic microspheres have been prepared.

Further analyses such as the influence of the magnetic amorphous microspheres on the blood, peritoneum cytometry and toxicity are currently in progress.

In conclusion, magnetic amorphous microspheres could be successfully used in biomedical applications such as immunomagnetic assay (especially dense liquids), for the detection of different biomolecules, or for occlusion of blood vessels with therapeutic intent (embolization therapy).

References

[1] W. Möller, G. Scheuch, K. Sommer, J. Heyder, J. Magn. Magn. Mater. 225 (2001) 8.
[2] R. Hasegawa, J. Magn. Magn. Mater. 100 (1991) 1.
[3] H. Chiriac, A.E. Moga, M. Urse, et al., J. Non-Cryst. Solids 250–252 (1999) 766.
[4] H. Chiriac, A.E. Moga, M. Urse, Patent No. RO113913B/1998.